

# Nucleation and Growth Synthesis of Siloxane Gels to Form Functional, Monodisperse, and Acoustically Programmable Particles\*\*

C. Wyatt Shields IV, Danping Sun, Kennita A. Johnson, Korine A. Duval, Aura V. Rodriguez, Lu Gao, Paul A. Dayton, and Gabriel P. López\*

Dedicated to Professor George M. Whitesides on the occasion of his 75th birthday

**Abstract:** Nucleation and growth methods offer scalable means of synthesizing colloidal particles with precisely specified size for applications in chemical research, industry, and medicine. These methods have been used to prepare a class of silicone gel particles that display a range of programmable properties and narrow size distributions. The acoustic contrast factor of these particles in water is estimated and can be tuned such that the particles undergo acoustophoresis to either the pressure nodes or antinodes of acoustic standing waves. These particles can be synthesized to display surface functional groups that can be covalently modified for a range of bioanalytical and acoustophoretic sorting applications.

**B**iofunctional, polymeric particles in suspension have been used to isolate proteins,<sup>[1]</sup> sort cells,<sup>[2]</sup> and deliver drugs, genes, or small molecules.<sup>[3]</sup> An emerging use of these particles is in acoustofluidic systems, which use standing pressure waves for rapid filtration,<sup>[4]</sup> sorting,<sup>[5]</sup> and flow cytometry.<sup>[6]</sup> While the majority of laboratory and commercial particles display positive acoustic contrast behavior by focusing along the nodes of an acoustic standing wave, we have shown that elastomeric silicone particles can display negative acoustic contrast behavior and can be used to isolate small bioanalytes and cells to the pressure antinodes for sorting.<sup>[1a,7]</sup> Previously, we have synthesized elastomeric particles using rapid homogenization techniques; however, these methods typically suffer from poor control over particle size and size dispersity.<sup>[7b]</sup> As

an alternative, we and other groups have synthesized elastomeric particles using microfluidics, which can provide narrow size distributions, but suffer from low particle production rates.<sup>[1a,8]</sup>

We have implemented methods for the nucleation and growth of alkoxy silane and silicon alkoxide monomers to develop a class of functional, monodisperse, and acoustically programmable (FMAP) particles that can be synthesized in bulk (Figure 1). These particles 1) can display ample surface groups (for example, vinyl and acrylate) for high-yield conjugations; 2) exhibit narrow size distributions (less than 15% CV); and 3) exhibit tunable acoustic behaviors (that is, positive or negative acoustic contrast factors,  $\phi$ ) for versatile manipulations in acoustofluidic systems. FMAP particles can display  $\phi > 0$  or  $\phi < 0$  behavior by migrating to the node(s) or antinodes of an acoustic standing wave, respectively. The  $\phi$  is dependent on the density and compressibility of the particle and its suspending fluid; particles with higher densities and

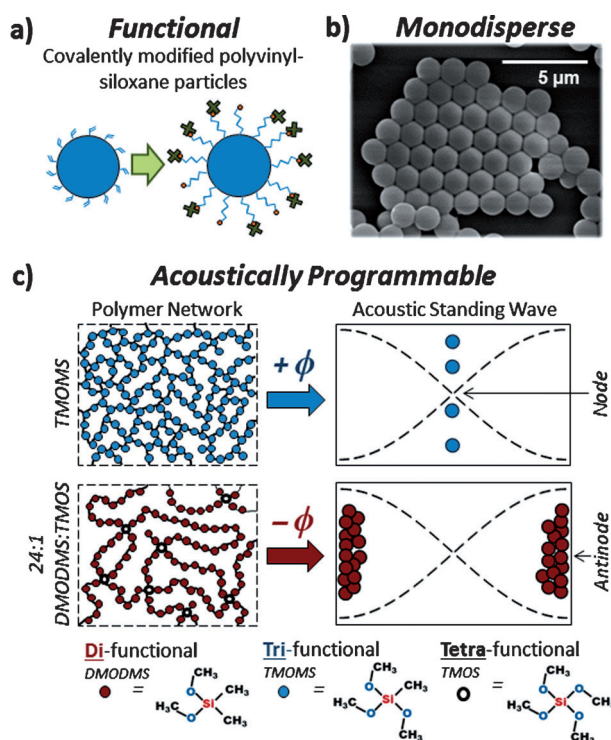


**Figure 1.** Siloxane-based particles formed by nucleation and growth synthesis can a) contain various functional groups (for example, hydroxy, vinyl, and acrylate) for surface modification, b) exhibit narrow size distributions, and c) display tunable acoustic properties.

[\*] C. W. Shields IV, D. Sun, Prof. G. P. López  
Department of Biomedical Engineering  
Duke University, Durham, NC (USA)  
E-mail: gabriel.lopez@duke.edu

C. W. Shields IV, Dr. K. A. Johnson, Dr. L. Gao, Prof. G. P. López  
NSF Research Triangle Materials Research Science and Engineering Center (USA)

Dr. K. A. Johnson, A. V. Rodriguez, Prof. P. A. Dayton  
Department of Biomedical Engineering  
University of North Carolina, Chapel Hill, NC (USA)

K. A. Duval, Dr. L. Gao, Prof. G. P. López  
Department of Mechanical Engineering and Materials Science  
Duke University, Durham, NC (USA)

[\*\*] This work was supported by the NSF's Research Triangle MRSEC (DMR-1121107) and an NSF Graduate Research Fellowship (1106401) to C.W.S. The authors thank Alexander A. Doinikov for his assistance with the theoretical considerations of particles in an acoustic field.

Supporting information for this article is available on the WWW under <http://dx.doi.org/10.1002/anie.201402471>.

bulk moduli relative to the fluid tend to focus along the pressure node(s), whereas particles with the opposite properties (for example, elastomeric particles in water) tend to focus along the pressure antinodes.<sup>[7b]</sup>

We used three variations of a nucleation and growth process to prepare particles from an assortment of alkoxy-silane and silicon alkoide monomers (for example, trimethoxymethylsilane (TMOMS), dimethoxymethylsilane (DMODMS), vinyltrimethoxysilane (VTMOS), vinylmethyl-dimethoxysilane (VMDMOS), 3-(trimethoxysilyl)propyl acrylate (AcTMOS), and tetramethyl orthosilicate (TMOS)). Each approach involves the hydrolytic cleavage of alkoide groups in the monomers followed by the uniform polycondensation of those monomers in an alkaline catalyst (see the Supporting Information for details).<sup>[9]</sup>

Approach I follows the Stöber process in which a small volume of monomers was added to water and a co-solvent.<sup>[10]</sup> The monomers underwent both hydrolysis and polycondensation after the addition of a catalyst. Approach II, which can be used to make relatively large (10  $\mu\text{m}$ ) particles, decouples the hydrolysis and polycondensation steps of Approach I by hydrolyzing the monomers at a low pH and later polymerizing those monomers at higher pH.<sup>[11]</sup> Approach III introduces a centrifugation step prior to polycondensation, which generates particles with the narrowest size distribution owing to the removal of large, non-uniform oligomers (Figure 2a).<sup>[12]</sup>

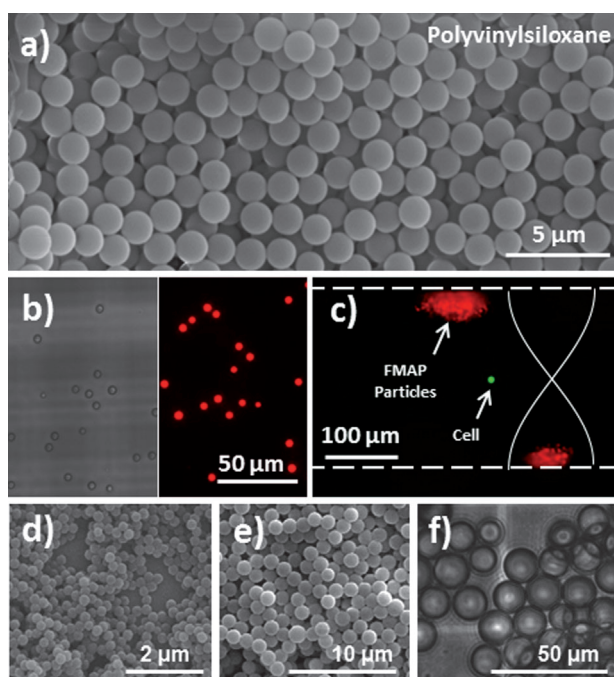


**Figure 2.** a) SEM image of particles synthesized from VTMOS. b) Bright-field (left) and fluorescence (right) images of Nile red-impregnated particles synthesized from a 96:1 molar ratio of DMODMS:TMOS. c) Particles from (b) and a mammalian cell (KG-1a, dyed green) focused along the antinodes and node of an acoustic standing wave, respectively (dashed white lines represent the walls of the microchannel). Particles synthesized from different concentrations of d,e) TMOMS and f) a 96:1 molar ratio of DMODMS:TMOS, displaying an average size of  $230 \pm 17$  nm,  $2.6 \pm 0.1$   $\mu\text{m}$ , and  $14.8 \pm 0.8$   $\mu\text{m}$ , respectively.

As necessary, we incorporated hydrophobic dyes (such as Nile red) into the particles (Figure 2b) for their visualization (for example, in the presence of calcein-dyed mammalian cells) in an acoustofluidic chip (Figure 2c). To illustrate the versatility of the nucleation and growth process, we provide examples of FMAP particles synthesized by all three approaches and highlight the properties of particles synthesized from TMOMS, VTMOS, and varying molar ratios of DMODMS:TMOS (8:1, 24:1, 48:1, 72:1, and 96:1).

By regulating the type of monomers, their concentration, and reaction time, we controlled the size of particles over a large range (230 nm to 14.8  $\mu\text{m}$ ; Figure 2d–f). We observed that particles with the narrowest size distribution (that is, the lowest size dispersity) were synthesized from TMOMS, VTMOS, or high molar ratios (96:1) of DMODMS:TMOS. To measure particle size, we used tunable resistive-pulse sensing (TRPS), which exploits the Coulter principle in a qNano device (IZON Science Ltd.).<sup>[13]</sup> Prior to sizing, particles were stabilized with surfactant (0.1 vol% F-108, Sigma) and diluted in 1xPBS. We found that: 1) particles synthesized from larger molar ratios of DMODMS:TMOS displayed smaller sizes; 2) particles synthesized from higher concentrations of monomer in water displayed larger sizes; and 3) particles synthesized with higher spin speeds during their growth exhibited smaller sizes (see the Supporting Information, Figure S2 and Tables S1–S3).

We synthesized particles containing different reactive functional groups (that is, vinyl and acrylate) by polymerizing functional monomers (for example, VTMOS and AcTMOS; see the Supporting Information for ATR-FTIR spectra). To examine their colloidal stability, we measured the zeta potential of these functional particles in 1xPBS (without adding surfactant) using the TRPS method (Figure 3a).<sup>[14]</sup> Particles made from 0.96 vol% VTMOS (average size:  $247 \pm 51$  nm) displayed an average zeta potential  $-36.2 \pm 3.2$  mV. By comparison, much larger particles made from 8.91 vol% TMOMS ( $1221 \pm 87$  nm) displayed an average zeta potential of  $-29.7 \pm 2.4$  mV. The zeta potential of these particles indicates moderate colloidal stability without surfactants.<sup>[14]</sup>

Next, we investigated the covalent modification of the surface of FMAP particles for the attachment of biomolecules. While we have shown that nonspecific physical adsorption can immobilize proteins on silicone particles for biosensing<sup>[1a]</sup> and cellular binding,<sup>[7a]</sup> covalent biofunctionalization provides a more stable means of attachment. We performed thermally initiated thiol–ene reactions on the surface of particles synthesized from a 24:1 molar ratio of VMDMOS:TMOS to immobilize a thiol-PEG<sub>70</sub>-biotin compound (Nanocs, Inc.; see the Supporting Information for details). We then incubated the biotinylated particles in fluorescent streptavidin (SA, 33 mM; Invitrogen) for 20 h and measured the adsorbed molecules of SA/particle using a flow cytometer (BD Accuri C6; Figure 3b). As controls, we analyzed the fluorescence of bare particles, bare particles incubated with SA, and biotinylated particles incubated with biotin-blocked SA.

The resulting peaks (or modes) in the number of SA molecules for particles nonspecifically adsorbed with SA, biotinylated particles adsorbed with biotin-blocked SA, and

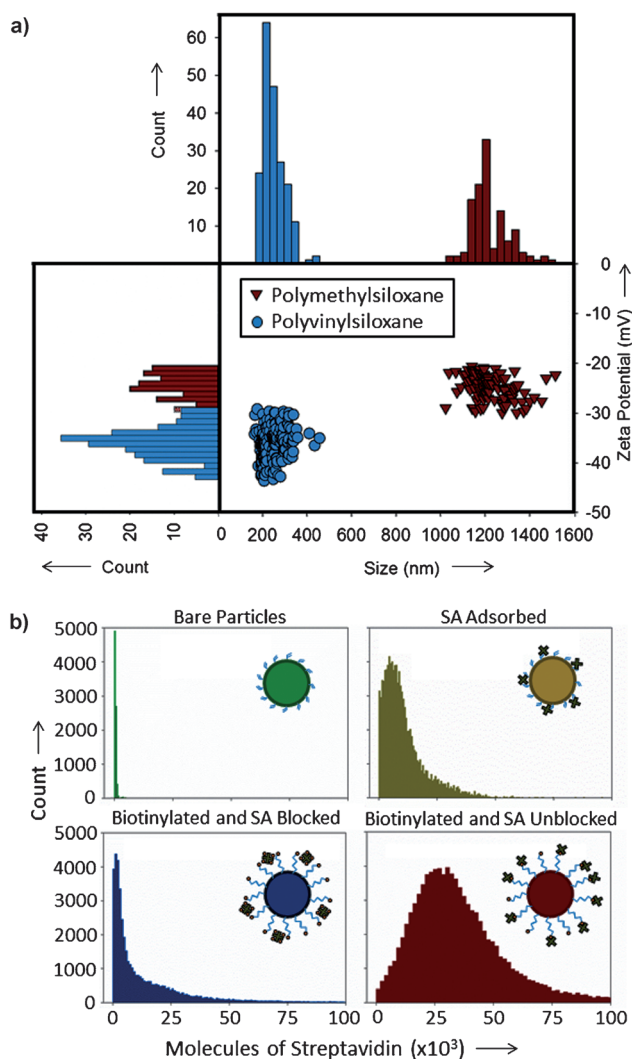


**Figure 3.** a) Zeta potential and size of particles made from TMOMS and VTOMS. b) Histograms of the number of adsorbed molecules of SA per particle as measured by a flow cytometer (particles synthesized from a 24:1 molar ratio of VMDOMS:TMOS). From top left to bottom right: bare particles, bare particles with adsorbed SA, biotinylated particles with adsorbed biotin-blocked SA, and biotinylated particles with adsorbed, unblocked SA.

biotinylated particles adsorbed with unblocked SA were measured to be approximately  $5 \times 10^3$ ,  $1 \times 10^3$ , and  $2.7 \times 10^4$ , respectively. The larger mode observed for the unblocked, biotinylated polyvinylsiloxane particles compared to the controls indicated that the SA adsorption was biospecific, which is an important hallmark for controlled biomolecular recognition at interfaces.<sup>[14]</sup>

We controlled the acoustic responsiveness of FMAP particles by selecting different molar ratios of alkoxysilane and silicon alkoxide monomers that could form different numbers of siloxane bonds. For example, particles synthesized from monomers that predominantly formed three (for example, TMOMS) or four (TMOS) siloxane bonds exhibited positive acoustic contrast behavior, and particles synthesized predominantly from monomers that form two siloxane bonds (DMODMS) exhibited negative acoustic contrast behavior.

The latter focusing behavior (that is, along the pressure antinodes) is useful because cells generally focus along the pressure node(s) (Figure 2c), allowing rapid, continuous sorting in acoustofluidic systems.<sup>[1a,7]</sup>

We synthesized six batches of particles from TMOMS and different molar ratios of DMODMS:TMOS, measured the displacement of each particle type in response to an acoustic traveling wave (1 MHz), and tracked their migration with a high speed camera (see the Supporting Information for details).<sup>[15]</sup> Using this method, we determined the acoustic radiation force acting on each of the particles, which allowed us to calculate their acoustic response parameter,  $\psi_p$ , by equating their acoustophoretic force with Stokes' drag force (see the Supporting Information for the full expression).<sup>[16]</sup> We then measured the densities ( $\rho_p$ ) of the particles to allow estimation of their compressibilities ( $\beta_p$ ) and their  $\phi_p$ . We found that particles migrated according to their composition, where particles synthesized from larger ratios of DMODMS:TMOS displayed a larger  $\psi_p$  and a more negative  $\phi_p$ . Figure 4 summarizes the data obtained for the particle set ( $\rho_p$ ,  $\beta_p$ ,  $\psi_p$ , and  $\phi_p$ ).

We then injected the same set of particles into an acoustofluidic microchip and measured their response to a standing wave under high-flow conditions ( $300 \mu\text{L min}^{-1}$ ). As indicated by their acoustic focusing profiles at a fixed location along the microchannel<sup>[8]</sup> (Figure 5), particles synthesized from larger ratios of DMODMS:TMOS (for example, 96:1) exhibited  $\phi < 0$  behavior and focused closer to the pressure antinodes than particles made from smaller mono-

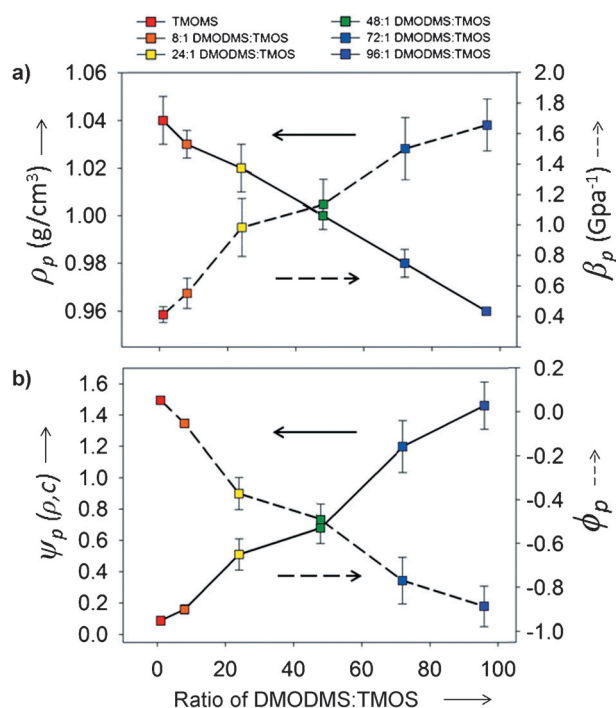


**Figure 4.** Properties of FMAP particles. a) Fundamental properties of particles by monomer composition: density,  $\rho_p$  (solid line, left axis) and compressibility,  $\beta_p$  (dashed line, right axis). b) Acoustic properties of particles by monomer composition: acoustic response parameter,  $\psi_p(\rho, c)$  (solid line, left axis), and acoustic contrast factor,  $\phi_p$  (dashed line, right axis; see Supporting Information for details).



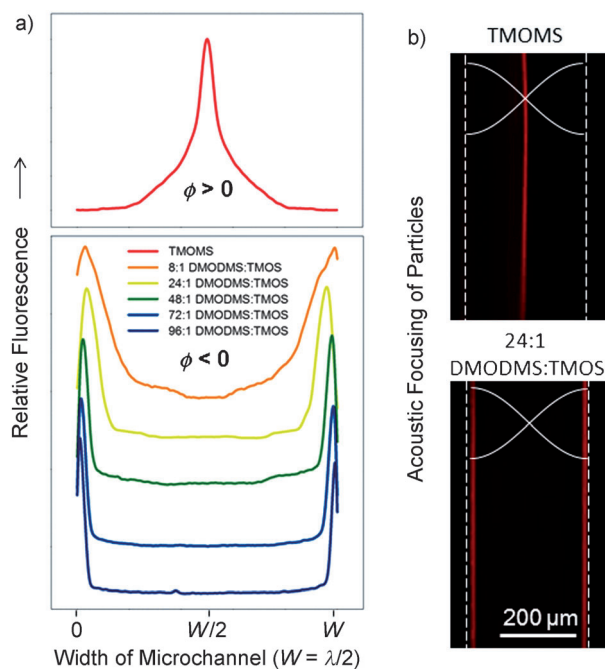


**Figure 5.** Evaluation of particles flowing through an acoustic standing wave. a) Fluorescence intensity profiles across the width of an acoustofluidic channel for different particle types flowing through the channel as shown in (b);  $300 \mu\text{L min}^{-1}$  flow rate;  $30 V_{pp}$  sinusoid waveform;  $2.96 \text{ MHz}$ ;  $\lambda \approx 500 \mu\text{m}$ . b) Micrographs of fluorescent particles flowing at the node (top) and antinodes (bottom) of an acoustic standing wave.

mer ratios (8:1). Moreover, particles synthesized from TMOMS exhibited  $\phi > 0$  behavior by focusing along the pressure node. The relative slope of their focusing profiles correlated with the calculated acoustic contrast factors, indicating this synthesis method can be used to program the acoustic properties of particles in both traveling and standing acoustic waves by their monomer composition.

In summary, we show that siloxane-based particles made by nucleation and growth can provide a precise means for programming particle size, surface functionality, and acoustic properties. These particles are useful for applications in bioanalytical acoustofluidics as well as other applications, as they are rapidly generated in bulk, are biofunctional, and are easily programmable.

Received: February 17, 2014

Revised: April 2, 2014

Published online: May 22, 2014

**Keywords:** acoustofluidics · biosensing · colloids · nucleation and growth · sol–gel

- [1] a) K. W. Cushing, M. E. Piyasena, N. J. Carroll, G. C. Maestas, B. A. López, B. S. Edwards, S. W. Graves, G. P. López, *Anal. Chem.* **2013**, *85*, 2208–2215; b) M. A. Nash, J. N. Waitumbi, A. S. Hoffman, P. Yager, P. S. Stayton, *ACS Nano* **2012**, *6*, 6776–6785.
- [2] a) S. Miltenyi, W. Muller, W. Weichel, A. Radbruch, *Cytometry* **1990**, *11*, 231–238; b) A. Lenshof, T. Laurell, *Chem. Soc. Rev.* **2010**, *39*, 1203–1217.
- [3] Y. Xia, B. Gates, Y. Yin, Y. Lu, *Adv. Mater.* **2000**, *12*, 693–713.
- [4] A. Lenshof, C. Magnusson, T. Laurell, *Lab Chip* **2012**, *12*, 1210–1223.
- [5] P. Augustsson, C. Magnusson, M. Nordin, H. Lilja, T. Laurell, *Anal. Chem.* **2012**, *84*, 7954–7962.
- [6] M. E. Piyasena, P. P. Austin Suthanthiraraj, R. W. Applegate, Jr., A. M. Goumas, T. A. Woods, G. P. López, S. W. Graves, *Anal. Chem.* **2012**, *84*, 1831–1839.
- [7] a) C. W. Shields IV, L. M. Johnson, L. Gao, G. P. López, *Langmuir* **2014**, *30*, 3923–3927; b) L. M. Johnson, L. Gao, C. W. Shields IV, M. Smith, K. Efimenko, K. Cushing, J. Genzer, G. P. Lopez, *J. Nanobiotechnol.* **2013**, *11*, 22.
- [8] W. J. Duncanson, T. Lin, A. R. Abate, S. Seiffert, R. K. Shah, D. A. Weitz, *Lab Chip* **2012**, *12*, 2135–2145.
- [9] G. H. Bogush, C. F. Zukoski IV, *J. Colloid Interface Sci.* **1990**, *142*, 1–18.
- [10] W. Stöber, A. Fink, E. Bohn, *J. Colloid Interface Sci.* **1968**, *26*, 62–69.
- [11] a) T. M. Obey, B. Vincent, *J. Colloid Interface Sci.* **1994**, *163*, 454–463; b) M. I. Goller, T. M. Obey, D. O. H. Teare, B. Vincent, M. R. Wegener, *Colloids Surf. A* **1997**, *123–124*, 183–193.
- [12] a) C. R. Miller, R. Vogel, P. P. Surawski, K. S. Jack, S. R. Corrie, M. Trau, *Langmuir* **2005**, *21*, 9733–9740; b) R. Vogel, P. P. Surawski, B. N. Littleton, C. R. Miller, G. A. Lawrie, B. J. Battersby, M. Trau, *J. Colloid Interface Sci.* **2007**, *310*, 144–150.
- [13] R. Vogel, G. Willmott, D. Kozak, G. S. Roberts, W. Anderson, L. Groenewegen, B. Glossop, A. Barnett, A. Turner, M. Trau, *Anal. Chem.* **2011**, *83*, 3499–3506.
- [14] D. Kozak, W. Anderson, R. Vogel, S. Chen, F. Antaw, M. Trau, *ACS Nano* **2012**, *6*, 6990–6997.
- [15] P. A. Dayton, J. S. Allen, K. W. Ferrara, *J. Acoust. Soc. Am.* **2002**, *112*, 2183–2192.
- [16] R. Barnkob, P. Augustsson, T. Laurell, H. Bruus, *Lab Chip* **2010**, *10*, 563–570.